

Histogram-Free Multicanonical Monte Carlo Sampling to Calculate the Density of States

Alfred C.K. Farris^{a,*}, Ying Wai Li^{b,*}, Markus Eisenbach^b

^a*Center for Simulational Physics, Department of Physics and Astronomy, The University of Georgia, Athens, GA 30602, U.S.A.*

^b*National Center for Computational Sciences, Oak Ridge National Laboratory, Oak Ridge, Tennessee 37831, U.S.A.*

Abstract

We report a new multicanonical Monte Carlo algorithm to obtain the density of states for physical systems with continuous state variables in statistical mechanics. Our algorithm is able to obtain a closed-form expression for the density of states expressed in a chosen basis set, instead of a numerical array of finite resolution as in previous variants of this class of MC methods such as the multicanonical sampling and Wang-Landau sampling. This is enabled by storing the visited states directly and avoiding the explicit collection of a histogram. This practice also has the advantage of avoiding undesirable artificial errors caused by the discretization and binning of continuous state variables. Our results show that this scheme is capable of obtaining converged results with a much reduced number of Monte Carlo steps, leading to a significant speedup over existing algorithms.

Keywords: Monte Carlo, statistical mechanics, density of states, algorithms

PROGRAM SUMMARY

Program Title: HistogramFreeMUCA

Licensing provisions: BSD 3-clause

Programming language: Python

Nature of problem:

This program implements a novel algorithm to obtain the density of states of a physical system, expanded in a chosen basis set. Unlike existing algorithms that return the density of states as a numerical array, this algorithm avoids binning of a continuous variable and is able to express the density of states as a closed-form expression. It is thus suitable for the study of the statistical mechanics and thermodynamic properties of physical systems where the density of a continuous state variable is of interest.

Solution method:

The new algorithm presented here is a special reweighting method in classical Monte Carlo approaches. In particular, it can be regarded as a descendant and a hybrid method closely related to the multicanonical method and Wang-Landau sampling.

Additional comments:

Most updated source code can be found at: <https://github.com/yingwaili/HistogramFreeMUCA>

1. Introduction

Monte Carlo (MC) methods are one of the major computational techniques in statistical physics for the study of finite temperature properties and thermodynamics of materials [1]. Traditional MC methods such as the Metropolis algorithm [2], an importance sampling method, works by generating a Markov chain of energy states E that obey the Boltzmann distribution, $e^{-E/k_B T}$, which describes the probability of finding the system at a certain energy state at a given temperature T . Thermodynamics properties are then calculated by averaging over the entire Markov chain after equilibration. A well-known limitation of the Metropolis method is the “critical slowing down” near phase transitions [3], where the correlation time diverges at the critical temperature T_C . Hence, simulations around and below T_C are simply impractical or unreliable to perform.

*Corresponding authors.

Email addresses: alfred.farris@uga.edu (Alfred C.K. Farris), yingwaili@ornl.gov (Ying Wai Li)

¹This manuscript has been authored by UT-Battelle, LLC under Contract No. DE-AC05-00OR22725 with the U.S. Department of Energy. The United States Government retains and the publisher, by accepting the article for publication, acknowledges that the United States Government retains a non-exclusive, paid-up, irrevocable, worldwide license to publish or reproduce the published form of this manuscript, or allow others to do so, for United States Government purposes. The Department of Energy will provide public access to these results of federally sponsored research in accordance with the DOE Public Access Plan (<http://energy.gov/downloads/doe-public-access-plan>).

Important breakthroughs were introduced by advanced techniques such as the reweighting methods, which allow for the procurement of a distribution function of properties. They can be used to obtain properties at a temperature other than the simulation temperature by “reweighting” the distribution function properly: umbrella sampling [4, 5], multihistogram method [6], multicanonical (MUCA) sampling [7, 8], and more recently Wang-Landau (WL) sampling [9, 10], all belong to this class of reweighting methods. Because of a special formulation of the sampling weights that control the acceptance probability, the random walks in these methods are not “trapped” in local minima as in Metropolis sampling. They are thus able to circumvent the critical slowing down problem. Among the reweighting methods, Wang-Landau sampling is proven to be quite robust because the simulation is performed *independent* of temperature. The resulting distribution function is essentially the density of states (DOS), i.e., the energy degeneracy of the system. Thus it reflects only the intrinsic properties defined by the Hamiltonian. The DOS allows for direct access to the microcanonical entropy, with which all the thermodynamics properties including the specific heat and free energy can be calculated. This feature is essential to enable a reliable study of phase transitions and critical phenomena, particularly at low temperatures.

With the advancement of high performance computers (HPC), it is now possible to combine Wang-Landau sampling with first-principles methods, e.g. density functional theory (DFT) [11, 12], to simulate finite temperature materials properties to a high accuracy that is comparable with experimental observations [13, 14, 15]. However, first-principles energy calculations are computationally intensive; and yet a reliable Wang-Landau sampling often needs a minimum of millions of MC steps (i.e. energy calculations) for one single simulation. The time required to finish a simulation is often measured in weeks or even months on one of the fastest supercomputers currently available. Such a huge computational cost is barely affordable. The type of scientific problems that can be practically solved by this approach are, for this reason, still very limited.

To address this problem, improvements of existing Monte Carlo algorithms are required. In general, two feasible strategies are available: one is the parallelization of existing algorithms, in which computational cost is spread over multiple computing units. Examples include parallel tempering [16, 17], parallel Wang-Landau sampling on a graphical processing unit (GPU) [18], replica-exchange Wang-Landau sampling [19, 20], and parallel multicanonical sampling [21, 22]. Another

strategy is to find ways to reduce the number of MC steps needed to complete a simulation. This is normally done by introducing tricks within the framework of existing algorithms; but the number of MC steps saved is often small.

In this work, we present a new multicanonical Monte Carlo algorithm that takes both strategies into account. Our scheme is readily parallelizable as in [21, 22] to exploit the power of current HPC architectures. In addition, our algorithm is able to attain comparable accuracy with Wang-Landau sampling, using only about 1/10 of the number of MC steps. This order of magnitude reduction in the number of energy evaluations is particularly crucial when first-principles methods are employed for calculating the energy. Moreover, for the very first time, our algorithm provides a viable means to obtain the density of states as a closed-form expression. The utility of this is twofold: Firstly, working with a closed-form expression during the simulation allows us to avoid using histograms to represent continuous variables, and in turn bypass systematic errors associated with the choice of the resolution for the order parameters, i.e., the bin width of the histogram or density of states as in multicanonical and Wang-Landau sampling. Thus, this framework will be of particular use when studying statistical mechanical models with continuous phase-space variables, e.g., the classical Heisenberg model, coarse-grained biopolymer models, Lennard-Jones fluids or clusters, which will be discussed in follow-on publications. Secondly, because we are able to obtain a closed-form expression, this algorithm will be particularly useful to fit the functional form of the density of states to aid theoretical studies.

This paper is extended based on the proceeding paper accepted in the Platform for Advanced Scientific Computing Conference (PASC’17) [23]. Here, we include a Python code to illustrate the implementation of our algorithm. We also added Appendix A to clarify the definitions and the use of the Kolmogorov-Smirnov test employed in our scheme, as it is a major factor affecting the behavior and the accuracy of the algorithm presented in this work.

2. Description of the algorithm

2.1. An overview

Our novel algorithm is inspired by previous multicanonical (MUCA) [7, 8] and Wang-Landau (WL) [9, 10] Monte Carlo methods. Therefore our algorithm shares many of its underlying principles with these earlier methods. The major advantage of our scheme over

the previous ones is that our algorithm, for the first time, provides a viable avenue to estimate a closed-form expression of the density of states in energy, denoted by $g(E)$. Here E stands for an energy the simulated physical system can realize. We assume an expansion for the natural log of $g(E)$ in terms of an orthonormal basis set $\{\phi_i(E)\}$ with each term weighted by the coefficient g_i :

$$\ln g(E) = \sum_{i=1}^N g_i \phi_i(E), \quad (1)$$

with N being the number of basis functions utilized in the expansion. The estimation of $g(E)$ will be improved iteratively later during the course of the simulation by a similarly defined, yet slightly modified, correction function $c(E)$:

$$\ln c(E) = \sum_{i=1}^N c_i \phi_i(E), \quad (2)$$

where c_i is the weighting coefficient for $\phi_i(E)$ in the correction.

The algorithm begins with an initial guess of $\tilde{g}(E) = 1$ (i.e., $\ln \tilde{g}(E) = 0$). In other words, it is a uniform distribution. Next, a series of Monte Carlo moves is performed and a Markov chain of k energies is generated to construct a data set $\mathcal{D} = \{E_1, E_2, \dots, E_j, \dots, E_k\}$ according to the following acceptance probability:

$$p(E_j \rightarrow E_{j+1}) = \min\left(\frac{\tilde{g}(E_j)}{\tilde{g}(E_{j+1})}, 1\right). \quad (3)$$

Note that the acceptance rule follows that of the Wang-Landau algorithm [9]. That is, if the trial energy E_{j+1} is rejected, the previous accepted state of the system should be recovered, but the associated energy E_j would be counted again as E_{j+1} . A Monte Carlo move is then performed on the reverted state to generate the next trial energy E_{j+2} .

After the data set \mathcal{D} is generated, it is used to find the correction $c(E)$ that improves the estimated density of states $\tilde{g}(E)$ such that:

$$\ln \tilde{g}(E) \rightarrow \ln \tilde{g}(E) + \ln c(E). \quad (4)$$

The details of obtaining the correction function $c(E)$ from the data set \mathcal{D} will be further described below in subsection 2.2. For now, assume that we have updated the estimated density of states $\tilde{g}(E)$ with $c(E)$ using Eq. (4). The simulation is then brought to the next iteration with \mathcal{D} and $\ln c(E)$ reset to empty or zero, respectively, while $\tilde{g}(E)$ will be kept unchanged and carried over to the next iteration as the new sampling weights. The process of generating the data set \mathcal{D} and obtaining the correction $c(E)$ is then repeated. The iteration repeats and

terminates when $\ln c(E) \rightarrow 0$. The DOS of the system is a fixed point of the iterative process when convergence is reached.

2.2. Obtaining the correction $c(E)$ from data set \mathcal{D}

The key of the above framework is to obtain a closed-form expression for the correction $c(E)$, or $\ln c(E)$ in the actual implementation of our algorithm. To do so, we must first obtain such an expression for the empirical cumulative distribution function (ECDF) of the data \mathcal{D} , from which $c(E)$ can be deduced.

2.2.1. Obtaining a closed-form expression for the empirical cumulative distribution function (ECDF)

We construct the ECDF following the scheme proposed by Berg and Harris [24], which we outline here. Recall that our data set \mathcal{D} is a collection of k energies generated from a Monte Carlo Markov chain. The energies are first sorted in ascending order:

$$\begin{aligned} \mathcal{D} &= \{E_1, E_2, \dots, E_j, \dots, E_k\} \\ &= \{E_{\pi_1}, E_{\pi_2}, \dots, E_{\pi_j}, \dots, E_{\pi_k}\}, \end{aligned} \quad (5)$$

where π_1, \dots, π_k is a permutation of $1, \dots, k$ such that $E_{\pi_1} \leq E_{\pi_2} \leq \dots \leq E_{\pi_j} \leq \dots \leq E_{\pi_k}$. If all E_{π_j} are different, the empirical cumulative distribution function (ECDF) is defined as:

$$\bar{F}(E) = \frac{j}{k}, \quad \text{for } E_{\pi_j} \leq E < E_{\pi_{j+1}}. \quad (6)$$

If multiple E_{π_j} 's have the same value, e.g., $E_{\pi_j} = E_{\pi_{j+1}} = \dots = E_{\pi_{j+l}}$, the ECDF would take a larger step:

$$\bar{F}(E) = \frac{j+l}{k}, \quad \text{for } E_{\pi_j} = E_{\pi_{j+1}} = \dots = E_{\pi_{j+l}} \leq E < E_{\pi_{j+l+1}}. \quad (7)$$

Assuming that the ECDF can be decomposed into two components:

$$\bar{F}(E) = F_0(E) + \bar{R}(E), \quad (8)$$

where $F_0(E) = (E - E_{\pi_1}) / (E_{\pi_k} - E_{\pi_1})$ is a straight line for $E \in [E_{\pi_1}, E_{\pi_k}]$, and $\bar{R}(E)$ defines the empirical remainder. The choice of $F_0(E)$ as a straight line is based upon the following observations: for traditional histogram methods, the ECDF plays the role of the cumulative histogram that can be constructed directly from the histogram $H(E)$. Nevertheless, in the continuous limit, the ECDF does not suffer from the binning effect. The derivative of the ECDF is then equivalent to the histogram in traditional methods: $H(E) = d\bar{F}(E)/dE$. In such schemes, obtaining a ‘‘flat’’ histogram is an indicator that the energy space is being sampled uniformly.

The sampling weights are continuously adjusted to direct the random walk from highly accessible states to rare events, either periodically in MUCA or adaptively in WL, to achieve this goal. Here, a ‘‘flat histogram’’ is equivalent to an ECDF with a constant slope.

The next task is to find a closed-form expression for the remainder $R(E)$ to fit the empirical data $\bar{R}(E)$. $R(E)$ signifies the deviation from the ideal (uniform) sampling, which will inform us on how to amend the weights to drive the random walks. It is expected that $R(E)$ will be related to the correction $c(E)$. Therefore, it is reasonable to assume that $R(E)$ can be similarly expanded in terms of an orthonormal basis set $\{\psi_i(E)\}$:

$$R(E) = \sum_{i=1}^m r_i \psi_i(E), \quad (9)$$

where m is the number of terms in the expression. The coefficients r_i can be then be found by:

$$r_i = \mathcal{N} \int_{E_{\pi_1}}^{E_{\pi_k}} R(E) \psi_i(E) dE, \quad (10)$$

with \mathcal{N} being a normalization constant dependent on the choice of the basis set $\{\psi_i(E)\}$. Note also that the basis set $\{\psi_i(E)\}$ needs to be able to satisfy the ‘‘boundary conditions’’ at E_{π_1} and E_{π_k} that $R(E_{\pi_1}) = R(E_{\pi_k}) = 0$, by definition. Since $R(E)$ is indeed an empirical function resulted from the ECDF, the integral in Eq. (10) is a simple numerical summation.

The remaining question is to determine the number of terms m in Eq. (9) to fit $\bar{R}(E)$ while avoiding overfitting. This is done by an iterative procedure starting from $m = 1$ where there is only one term in the sum. A statistical test is then performed to measure the probability p that this $R(E)$ is a ‘‘good’’ fit to $\bar{R}(E)$. That is, p is the probability of obtaining the empirical remainder $\bar{R}(E)$ if the data is generated according to the distribution specified by $R(E)$. We follow the suggestion of [24] and use the Kolmogorov-Smirnov test [25, 26] (see Appendix A for details), but other statistical tests for arbitrary probability distributions can also be used. If $p < 0.5$, we increase m to $m + 1$ and repeat the statistical test, until $p \geq 0.5$ is reached. The number of terms m is then fixed at this point. Note that in principle, increasing m further would result in a ‘‘better fit’’ and thus a larger p . However, it is not preferable because it increases the risk of over-fitting a particular data set and would be difficult to correct through latter iterations. Thus we choose the criterion $p \geq 0.5$ to keep the expression as simple as possible, and to maintain some levels of stability against noise.

With the expression of $R(E)$, a closed-form approximation of the ECDF can then be obtained:

$$F(E) = F_0(E) + R(E). \quad (11)$$

2.2.2. From ECDF $F(E)$ to the correction $c(E)$

Finally, the expression of $F(E)$ in Eq. (11) is used to obtain the correction $c(E)$ (or $\ln c(E)$ in practice). Recall the definition of the cumulative distribution function (CDF) for a continuous variable, which can be constructed from the probability density function. They are, respectively, equivalent to $F(E)$ and $H(E)$:

$$F(E) = \int_{-\infty}^E H(E') dE'. \quad (12)$$

Combining Eqs. (11) and (12) and taking derivatives of both sides to obtain $H(E)$ yields:

$$\begin{aligned} H(E) &= \frac{dF(E)}{dE} = \frac{dF_0(E)}{dE} + \frac{dR(E)}{dE} \\ &= \frac{1}{E_{\pi_k} - E_{\pi_1}} + \sum_{i=1}^m r_i \frac{d\psi_i(E)}{dE}. \end{aligned} \quad (13)$$

As in traditional multicanonical sampling methods, the histogram $H(E)$ is used to update the estimated density of states $\tilde{g}(E)$, hence the sampling weights for the next iteration. Observe that the first term in Eq. (13) is just a constant independent of the value of E , it can be safely omitted in the correction. Thus, we choose to write the log of the correction using part of the histogram (taking only the second term in Eq. (13)):

$$\ln c(E) = \sum_{i=1}^m r_i \frac{d\psi_i(E)}{dE}, \quad (14)$$

which, in our special case, has the same form as Eq. (2) with

$$c_i \phi_i(E) = r_i \frac{d\psi_i(E)}{dE} \quad \text{and} \quad N = m.$$

In general, we need to ensure that $\frac{d\psi_i(E)}{dE}$ can be expanded in terms of $\{\phi_j(E)\}$, i.e.,

$$\frac{d\psi_i(E)}{dE} = \sum_j p_{ij} \phi_j(E).$$

Finally, the estimated density of states $\tilde{g}(E)$ is updated using Eq. (4).

2.3. A note on the update of the density of states

There is a major difference between our scheme and the traditional MUCA algorithm in the way the

density of states $\tilde{g}(E)$ gets updated. Effectively, our scheme updates $\tilde{g}(E)$ using $\exp(\Delta H(E))$ (where $\Delta H(E)$ denotes the deviation of the histogram $H(E)$ from uniform sampling, i.e., a “flat” histogram), whereas traditional MUCA updates $\tilde{g}(E)$ using the histogram $H(E)$ itself directly. Our scheme is therefore more responsive and proactive in adjusting the sampling weights, and thus $\tilde{g}(E)$, to guide the random walker to achieve uniform sampling.

3. Test case: numerical integration

The algorithm was originally designed with the motivation of sampling physical systems with a continuous energy domain. Yet, as the majority of these systems do not have a closed-form solution, it is difficult to quantify the accuracy of the algorithm. We thus apply it to perform numerical integration using the scheme suggested by Ref. [27] as a proof-of-principle.

Note, however, that our method is not meant to be an efficient algorithm for performing numerical integration. As pointed out in Ref. [27], there is a one-to-one correspondence between numerical integration and simulating an Ising model when put under the Wang-Landau sampling framework. This applies to our algorithm too and as long as we choose an integrand that is continuous within the interval $[y_{\min}, y_{\max}]$, it is equivalent to the situation of having a continuous energy domain for a physical system. Moreover, numerical integration is indeed a more stringent test case for our algorithm (and other histogram MC methods such as Wang-Landau sampling in general), because the “density of states” $g(y)$ is usually more rugged than the density of states of a real physical system.

If one can find an expression for the normalized $g(y)$, which measures the portion of the domain within interval $[a, b]$ corresponding to a certain value of y , then the integral can be found by summing the “rows” up (multiplied by the value of y) instead of the columns in the following manner:

$$I = \int_a^b y(x)dx = \int_{y_{\min}}^{y_{\max}} g(y)ydy. \quad (15)$$

Note that $g(y)$ needs to be normalized such that

$$\int_{y_{\min}}^{y_{\max}} g(y)dy = b - a. \quad (16)$$

We apply our algorithm to perform the following integration where the exact integral is known:

$$I = \int_{-2}^2 x^2 dx = \frac{16}{3} = 5.33333 \dots, \quad (17)$$

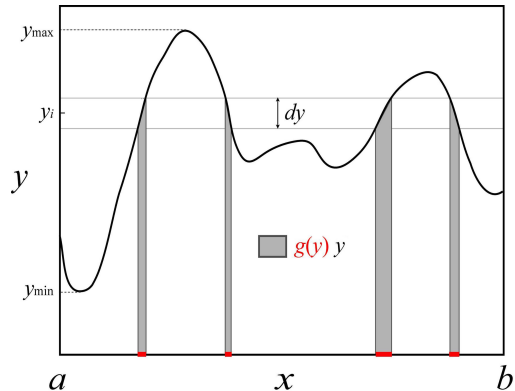


Figure 1: A schematic diagram showing the numerical integration notations. The red regions on the x -axis marked the portion within the interval $[a, b]$ that gives a certain value y . All the areas shaded in grey add up to give $g(y)y$.

and the “density of states” $g(y)$ can be expressed analytically:

$$g(y) = \frac{2(2 - \sqrt{y})}{y} \quad \text{for } y > 0. \quad (18)$$

We use a Fourier sine series as the basis set $\{\psi(E)\}$ to fit the remainder $R(E)$, and therefore a Fourier cosine series as the basis set $\{\phi(E)\}$ for constructing the correction $\ln c(E)$ and updating the density of states $\ln g(E)$. Moreover, we employ the Kolmogorov-Smirnov test in the $R(E)$ fitting step to determine if the expression obtained is a good fit to the dataset \mathcal{D} , using a criterion of $p = 0.5$. The experiment is done for different numbers of data in the data set, with $k = 250, 500, 1000$ and 2000 .

We note that the Fourier sine and cosine series are not well suited basis sets for this problem due to their oscillatory properties. Yet the algorithm works surprisingly well. In Figure 2, we show a resulting density of states, $g(y)$, compared to that obtained using Wang-Landau sampling. The fluctuations of our $g(y)$ fall within the statistical noise of the WL density of states.

The values of the estimated integral at different iterations for $k = 500$ and $k = 1000$ are shown in Figures 3 and 4, respectively.

We observe that the number of data points k in a data set within an iteration plays an important role in the accuracy. Both under-fitting from insufficient data and over-fitting from excessive data would produce inaccurate results. In both Figures 3 and 4, most estimated integrals agree with the exact value to within the error bars. No systematic correlation with the number of iterations is observed for either the estimated values of the integral or the magnitude of the error bars. Using

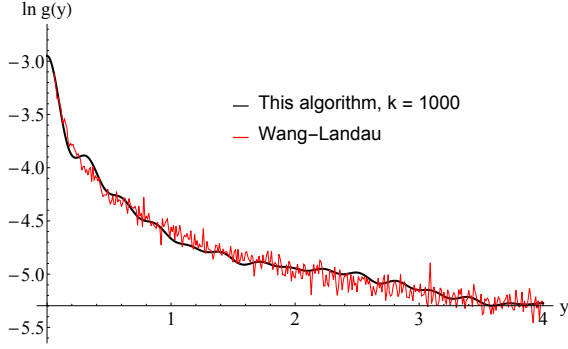


Figure 2: Density of states $g(y)$ at the 120th iteration, obtained using 1000 data points in a data set (black curve), a total of 1.2×10^5 MC steps are used. It is compared to a final $g(y)$ obtained using Wang-Landau sampling (red curve); this particular run requires 1.1×10^6 MC steps to complete. The DOS obtained from our algorithm is significantly smoother, yet its fluctuations fall within the statistical noise of the Wang-Landau DOS.

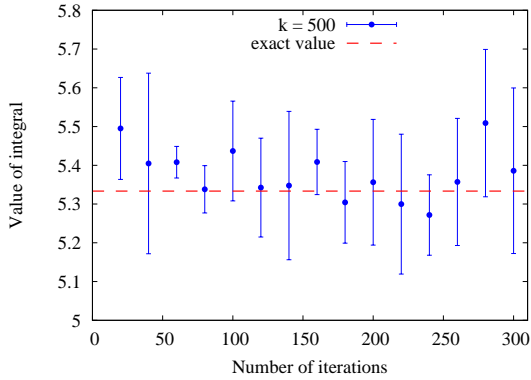


Figure 3: Integral of x^2 over $x \in [-2, 2]$, obtained using 500 data points in a data set. Error bars are obtained from five independent runs.

$k = 500$ or $k = 1000$ does not seem to result in significant differences in the estimated value of the integral. However, if we extend the studies and use fewer or more data points in the data set \mathcal{D} , we observe different behavior as shown in Figure 5. For the $k = 250$ case, the integral is slightly overestimated at the first 200 iterations or so. The percent errors fall back to within the same ranges as in the $k = 500$ and $k = 1000$ cases later. This is reasonable because as the number of iterations increases, more data are taken to correct the estimated density of states.

However, the integral is, unexpectedly, systematically underestimated for the $k = 2000$ case. We also observe that the number of terms in the expression of $R(E)$ and eventually $\ln g(E)$ generally increases with the number k (Table 1). A larger number of data results in a more de-

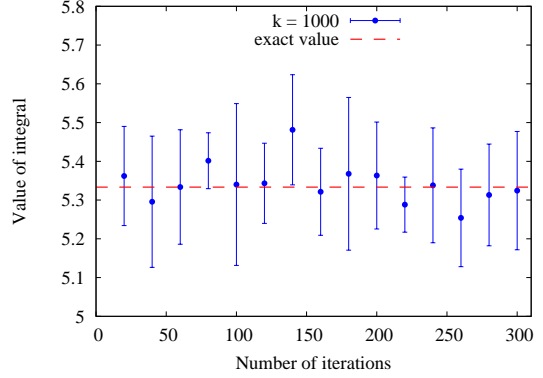


Figure 4: Integral of x^2 over $x \in [-2, 2]$, obtained using 1000 data points in a data set. Error bars are obtained from five independent runs.

tailed fitting of the DOS, hence more terms are used in the construction of the correction. Unfortunately, there is also a higher risk of fitting the noise “too well”, causing an over-fitting of the data set (this is due to the dependence of the KS test on the number of data points in a data set - see Appendix A for more details). On the other hand, using too few data points (such as $k = 250$) results in larger fluctuations in the values of the integral as well as in the number of terms N in the expression. From our observations, using about $k = 1000$ data points in a data set is the safest and it strikes a good balance between under-fitting (or even mal-fitting) and overfitting.

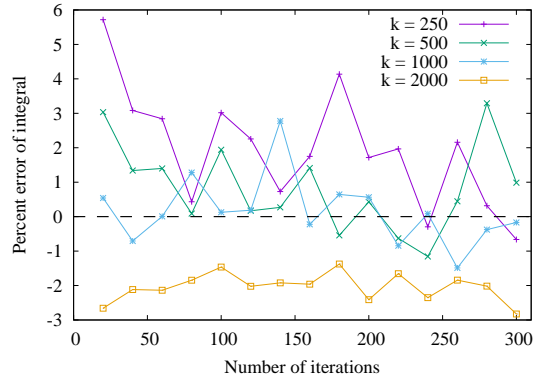


Figure 5: Percent errors of the averaged estimated integrals at different iterations using various numbers of data points k in a data set. The integrals for all cases are averaged over five independent runs. Except for $k = 2000$, all other cases converge to the exact value eventually with small errors (within $\pm 1\%$).

Note that the above experiments complete within hundreds of iterations. Considering $k = 1000$ data

k	N
250	19.4 ± 14.6
500	17.8 ± 6.1
1000	29.6 ± 4.3
2000	58.2 ± 13.0

Table 1: Averaged number of basis functions (N) for different number of data points (k) in each data set. The average values and errors are obtained from five independent runs. The number N is determined within the algorithm, at which the statistical test reaches $p \geq 0.5$.

points in an iteration, the total number of MC steps needed is of the order of 10^5 . Comparing to the order of 10^6 MC steps in Wang-Landau sampling, our scheme is more efficient and it saves about $10\times$ MC steps. The reason is that when we correct the estimated DOS (i.e., sampling weights), the correction is constructed to drive the random walk *intentionally* to achieve uniform sampling, or a “flat histogram”, as opposed to an incremental correction using the histogram as in MUCA or WL sampling. We believe that our correction scheme can also be applied to simple models with discrete energy levels and yields significant speedup.

4. An improved scheme for better convergence

While the results above showed that our proposed scheme is successful, one problem is that it is still difficult to determine whether convergence has been reached. Here, we suggest a possible way to improve the quality of the results with two slight modifications to the original scheme.

Firstly, when determining the number of terms for the remainder $R(E)$ (m in Eq. (9)), the original scheme starts from $m = 1$ and increments it to $m + 1$ sequentially until the statistical test gives a score of $p \geq 0.5$. We observe that this practice very often results in the update of the first few coefficients only. A remedy to it is that after the number m is determined in the first iteration, in the later iterations we propose random permutations of the terms for the expansion rather than adding the terms sequentially. The statistical test is still used to terminate the iteration as before. This way, every coefficient will have a roughly equal chance to get updated and refined.

Secondly, since the correction in Eq. (14) will drive the random walker in a way to achieve uniform sampling, we observe that it is beneficial to use a milder correction update to drive the random walker at a smaller step at a time. To do so, we rewrite Eq. (14) with a pre-factor s to take only a portion of $R(E)$ as the correction:

$$\ln c(E) = s \sum_{i=1}^m r_i \frac{d\psi_i(E)}{dE}. \quad (19)$$

With these two small modifications, we revisited the integration problem using $k = 1000$ data points in the data set (Figure 6). The integral values in the first few dozens of iterations deviate more from the exact value compared to the original scheme, but it converges slowly to the exact value with a much clearer convergence signal. In this example, one may terminate the simulation after e.g. the 150th iteration. Another clear improvement is that the error bar for each final answer is much reduced compared to the original scheme, which indicates that the improved scheme is able to give more precise results.

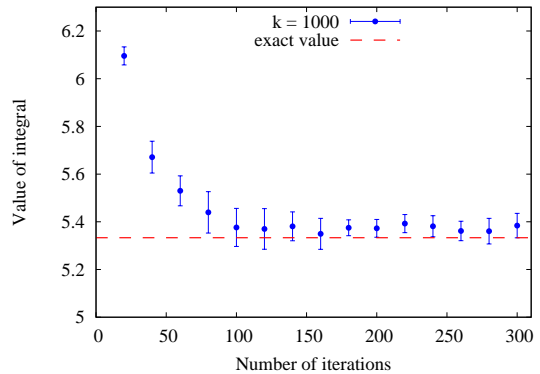


Figure 6: Integral of x^2 over $x \in [-2, 2]$, obtained using 1000 data points in a data set and the improved scheme with a milder correction with the pre-factor $s = 0.25$. Error bars are obtained from five independent runs.

5. Further improvements

Our scheme is general in the nature that the expression of the DOS, $g(E)$, is not restricted to the Fourier form above, as long as there is a way to formulate the correction $c(E)$ and the update formula. Obviously, the quality of the resulting density of states depends heavily on the choice of an appropriate basis set. While the plane wave basis used in the present study allowed us to implement a prototype of our algorithm without major effort, it suffers from serious issues that will require the choice of more suitable basis sets. In particular, local improvements to the density of states in a limited region of the domain should not introduce changes in regions far away. Also, the density of states often spans a wide range of values; indeed the density of states for the integration example possesses a singularity at the domain

boundary. Thus a more suitable, localized, basis set will greatly improve the convergence and accuracy of our method.

Although we present our method as a serial algorithm so far, we stress its parallelization is conceptually straight-forward. Since the generation of data points (which is the energy evaluations for a physical system) can be done independently by distributing the work over different processors, simple “poor-man’s” parallelization strategy would already guarantee significant speedup in both strong and weak scaling.

6. Conclusions

In this paper, we have presented a new Monte Carlo algorithm for calculating probability densities of systems with a continuous energy domain. The idea is inspired by combining ideas from the works of Wang and Landau [9, 10], Berg and Neuhaus [7, 8], as well as Berg and Harris [24]. Nevertheless, our algorithm does not make use of an explicit histogram as in traditional Wang-Landau or multicanonical sampling. It is thus possible to avoid discrete binning of the collected data. This histogram-free approach allows us to obtain the estimated probability density, or the density of states, as a closed-form expression.

We have demonstrated the application of our algorithm to a stringent test case, numerical integration. Even with the sub-optimal Fourier sine and cosine basis sets, our current algorithm is already capable of giving reasonable results. An important point to note is that our algorithm requires much *fewer* number of Monte Carlo steps to finish a simulation. It is enabled by the novel way we proposed to correct the estimated density of states, and thus the sampling weights, where the random walk is directed consciously to achieve uniform sampling. This is essential for decreasing the time-to-resolution ratio of a simulation, especially for complex systems where the computation time is dominated by energy evaluations.

The numerical integration test case provides useful insights into improving the algorithm. Possible improvements include the use of a basis set with local support and parallelization over energy calculations. The choice of basis set will have significant influence on the convergence behavior and the correctness of the simulation, but it often depends on the system of interest. In general, choosing a basis set with compact support would help by enabling local updates to the density of states, thus avoiding artificial sampling barriers. Our ongoing work includes all the possibilities for perfecting the algorithm, as well as its application to simula-

tions of physical systems to solve real-world scientific problems.

7. Computer Code

The following provides an overview of the code, a guide to running the code, and a detailed description of all program files.

7.1. Overview of the Computer Code

The associated computer code, written in Python 3.6, consists of a “main” program file - `binlessMUCA.py`, a sample input file - `input.txt`, and all necessary sub-routines to reproduce the results from the original and improved versions of the sampling scheme discussed in this manuscript. In addition to Python 3.6, Numpy, Sympy, and Matplotlib must be installed in order to run the code. The code can then be run from the terminal via: `$ python binlessMUCA.py input.txt`, where `input.txt` is an input file that is required as a command line argument. This input file must contain the following:

- i. random number seed (can be specified or generated randomly)
- ii. the function to integrate, $y(x)$
- iii. integration limits, a and b
- iv. number of points in the data set, k
- v. maximum terms in the basis set expansion (maximum value of m allowed)
- vi. the Kolmogorov-Smirnov cutoff probability, p
- vii. maximum number of iterations
- viii. desired sampling scheme (original scheme described in Section 2, or improved scheme described in Section 4 with associated pre-factor s)

One important note is that if the Kolmogorov-Smirnov probability is not satisfied within the specified maximum number of basis terms, the program will terminate and need to be restarted. In addition to the required input parameters, there are options to display certain plots during the simulation; these can be turned off or on by setting the associated variables to 0 or 1, respectively. The program outputs the random number seed and the estimate for the integral after each iteration. It terminates once the last iteration is completed.

7.2. Description of Subroutines

All necessary subroutines are included in `.py` files according to their functionality:

`binlessMUCA.py` is the main program file. It reads the input file and contains the main sampling loop that

updates the estimate for the density of states after each iteration, and terminates after the specified maximum iteration number.

`getExtrema.py` finds the global minimum and maximum of the input function over the interval defined by the integration limits.

`dataSetMethods.py` contains subroutines to construct the basis sets for the remainder and density of states, fill the data sets by randomly sampling the input function according to the acceptance probability in Eq. (3), and construct the empirical CDF and empirical remainder.

`correction.py` contains subroutines to find the closed-form approximation for the empirical remainder at each iteration by using the Fourier transform to find expansion coefficients (and thus correction coefficients) and the Kolmogorov-Smirnov probability to terminate the expansion. This file includes both the original and improved methods of obtaining the correction.

`KS.py` contains the subroutine to compute the Kolmogorov-Smirnov probability following the computer code in [24], which uses the asymptotic expansion from [28]. See Appendix A for details regarding the KS test.

`integrate.py` computes the integral based on the current estimate of the density of states.

`plotMethods.py` contains subroutines to plot certain physical quantities during the simulation.

Appendix A: The Kolmogorov-Smirnov Test

The Kolmogorov-Smirnov (KS) statistical test [25, 26] is used as the criterion to determine the number of terms in $c(E)$ and to terminate an iteration. Thus, it is essential to understand its behavior and to be aware of various subtleties in order to quantify its effects on the accuracy of the final results and to avoid errors.

All variants of the KS test return a probability, P , that the maximum distance between two cumulative distribution functions (CDF's), $\Delta = \sup |F_1(x) - F_2(x)|$, exceeds a predetermined value ε [29]. Nevertheless, there are different ways to define and compute P .

The first distinction gives rise to the one- and two-sided tests. The one-sided test will give two slightly different results depending on how the empirical CDF is defined - whether the data points are counted in the

previous step or the next step. This amounts to computing how much the CDF's differ in one direction - either above or below. The two-sided test uses the absolute maximum deviation, regardless of direction. In other words, it combines the results from both one-sided KS tests and returns the smaller probability. In our work we have used the two-sided test.

There exists an asymptotic expansion for the CDF of the two-sided KS statistic when the number of data points $k \rightarrow \infty$. If the two functions $F_1(x)$ and $F_2(x)$ are from the same distribution, the probability of the quantity $\sqrt{k}\Delta$ being smaller than or equal to a certain value z is [25]:

$$\lim_{k \rightarrow \infty} \mathbb{P}(\sqrt{k}\Delta \leq z) = 1 - 2 \sum_{j=1}^{\infty} (-1)^{j-1} e^{-2j^2 z^2}. \quad (20)$$

Substituting $z = \sqrt{k}\varepsilon$, we obtain the asymptotic expansion for the probability of Δ being larger than ε :

$$\begin{aligned} P &= \lim_{k \rightarrow \infty} \mathbb{P}(\Delta > \varepsilon) = 1 - \lim_{k \rightarrow \infty} \mathbb{P}(\Delta \leq \varepsilon) \\ &= 2 \sum_{j=1}^{\infty} (-1)^{j-1} e^{-2j^2 \varepsilon^2 k}. \end{aligned} \quad (21)$$

To apply the above results to our problem, we reverse the logic and reason that if we observe the maximum difference in the CDF's, Δ_{obs} , from our data points, i.e., $\varepsilon = \Delta_{\text{obs}}$, P can then be interpreted as the probability (level of confidence) of F_1 and F_2 coming from the same distribution [30]. A modification to the formula that replaces k with a modified form S_k was later introduced for the computation of the KS statistic instead of the use of numerical tables [28]. Therefore ²,

$$P = 2 \sum_{j=1}^{\infty} (-1)^{j-1} e^{-2j^2 \Delta_{\text{obs}}^2 S_k}, \quad (22)$$

where $S_k = \left(\sqrt{k} + 0.12 + \frac{0.11}{\sqrt{k}} \right)^2$.

The second distinction also impacts the way the probability measure is computed. The one-sample test computes the probability that a *single* data set of size N_{D1} was drawn from a specified, continuously defined probability distribution. The two-sample test computes the probability that *two* data sets of size N_{D1} and N_{D2} , respectively, were drawn from the same underlying, unspecified probability distribution. The asymptotic expansion for the two-sided test in Eq. (22) depends on the

²We note that in Ref. [29], there are errors with the formulae in Eq. (2.148) on Page 98. The implementation in the Fortran code, `kolm2_as.f`, is nevertheless correct, which is the same as Eq. (22) here.

number of data points, k , in the data set(s). In the case of the one-sample test, $k = N_{D1}$. However, the two-sample test uses an *effective* number of points given by:

$$k = \frac{N_{D1} \cdot N_{D2}}{N_{D1} + N_{D2}}. \quad (23)$$

The implications of using an effective number of points becomes apparent through analysis of the computed probability as a function of $\sup|F_1(x) - F_2(x)|$. Figure 7 shows how the KS probability changes for the one- vs. two- sample tests for 1000 data points, where the two-sample test uses an effective number of data points, $k = 500$, given by Eq. (23) with $N_{D1} = N_{D2} = 1000$. This figure indicates that the KS two-sample test, where each of the two data sets contains the same number of points as a single data set used with a one-sample test, results in a more lenient probability measure. Figure 8 shows how the one-sample KS probability changes as a function of the size of the data set. From this figure, it is apparent that decreasing the number of data points also decreases the stringency of the probability measure. In both figures, the solid line without symbols represents the same “baseline” for comparison to the other curves: a one-sample KS test with data set of size $k = 1000$. Interesting to note is that the two-sample test for two data sets of size $N_{D1} = N_{D2} = 1000$ produces exactly the same KS probability curve as does an $k = 500$ one-sample test: the dotted curve in Figure 7 and the line with squares in Figure 8 line up exactly. Thus, using the two sample test has the same effect as decreasing the size of the data set; i.e., both make the probability measure more lenient.

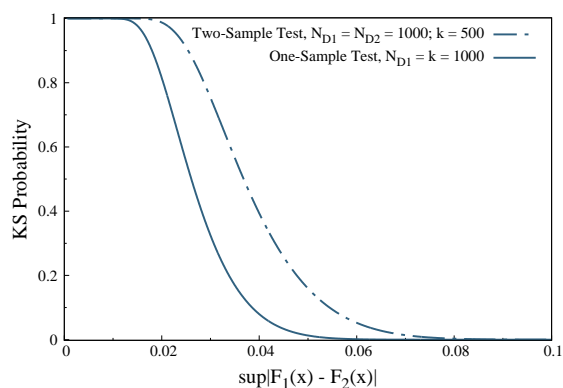


Figure 7: Comparison of the probability for the one- and two-sample KS tests as a function of the maximum distance between CDF's for data set(s) of size $N_{D1} = N_{D2} = 1000$. The *effective* number of data points k for the two sample test is given by Eq. (23).

The above analysis shows the importance of understanding which variant of the KS test a given scien-

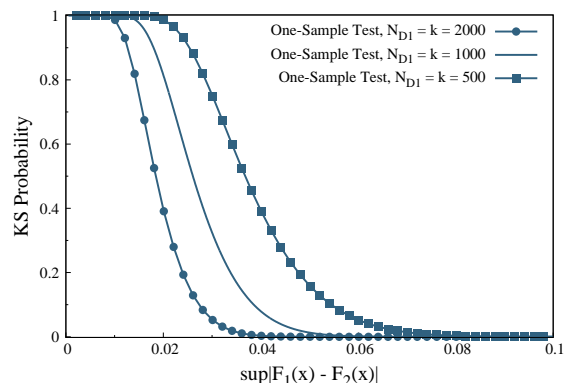


Figure 8: Comparison of the one-sample KS test probability as a function of the maximum distance between CDF's for data sets of different sizes.

tific computing package implements. The probability that the KS test returns is heavily reliant on k , and thus the results are heavily dependent on the particular implementation of the KS test. These subtleties must be understood in order to use the KS test correctly. The results shown in Section 3 were obtained by using the KS statistical test provided in the Mathematica software package [31]. However, the way to compute the probability measure is not specified in the documentation. In our Python code, we use the one-sample test. The default value of the Kolmogorov-Smirnov cutoff probability is set to be $p = 0.17$ in order to reproduce comparable probability measure as Mathematica (which uses the two-sample test and $p = 0.5$).

Acknowledgements

The authors would like to thank T. Wüst and D. M. Nicholson for constructive discussions. This research was sponsored by the Laboratory Directed Research and Development Program of Oak Ridge National Laboratory, managed by UT-Battelle, LLC, for the U. S. Department of Energy. This project was supported in part by an appointment to the Science Education Programs at Oak Ridge National Laboratory, administered by ORAU through the U.S. Department of Energy Oak Ridge Institute for Science and Education. This research used resources of the Oak Ridge Leadership Computing Facility, which is supported by the Office of Science of the U.S. Department of Energy under contract no. DE-AC05-00OR22725.

References

- [1] D. P. Landau, K. Binder, *A Guide to Monte Carlo Simulations in Statistical Physics*, 4th Edition, Cambridge University Press, 2014. doi : 10.1017/CB09781139696463.
- [2] N. Metropolis, A. W. Rosenbluth, M. N. Rosenbluth, A. H. Teller, E. Teller, *J. Chem. Phys.* 21 (6) (1953) 1087–1092.
- [3] P. C. Hohenberg, B. I. Halperin, *Rev. Mod. Phys.* 49 (3) (1977) 435–479.
- [4] C. H. Bennett, *J. Comput. Phys.* 22 (2) (1976) 245–268.
- [5] G. M. Torrie, J. P. Valleau, *J. Comput. Phys.* 23 (2) (1977) 187–199.
- [6] A. M. Ferrenberg, R. H. Swendsen, *Phys. Rev. Lett.* 63 (12) (1989) 4.
- [7] B. A. Berg, T. Neuhaus, *Phys. Lett. B* 267 (2) (1991) 249–253.
- [8] B. A. Berg, T. Neuhaus, *Phys. Rev. Lett.* 68 (1) (1992) 9–12.
- [9] F. Wang, D. P. Landau, *Phys. Rev. Lett.* 86 (10) (2001) 2050–2053.
- [10] F. Wang, D. P. Landau, *Phys. Rev. E* 64 (5) (2001) 056101.
- [11] P. Hohenberg, W. Kohn, *Phys. Rev.* 136 (3B) (1964) B864–B871.
- [12] W. Kohn, L. J. Sham, *Phys. Rev.* 140 (4A) (1965) A1133–A1138.
- [13] M. Eisenbach, C.-G. Zhou, D. M. Nicholson, G. Brown, J. Larkin, T. C. Schulthess, in: *Proceedings of the Conference on High Performance Computing Networking, Storage and Analysis, SC '09*, ACM, New York, NY, USA, 2009, pp. 64:1–64:8.
- [14] M. Eisenbach, D. M. Nicholson, A. Rusanu, G. Brown, *J. Appl. Phys.* 109 (7) (2011) 07E138.
- [15] S. N. Khan, M. Eisenbach, *Phys. Rev. B* 93 (2) (2016) 024203.
- [16] R. H. Swendsen, J.-S. Wang, *Phys. Rev. Lett.* 57 (21) (1986) 2607–2609.
- [17] K. Hukushima, K. Nemoto, *J. Phys. Soc. Jpn* 65 (6) (1996) 1604–1608.
- [18] J. Yin, D. P. Landau, *Comput. Phys. Commun.* 183 (8) (2012) 1568–1573.
- [19] T. Vogel, Y. W. Li, T. Wüst, D. P. Landau, *Phys. Rev. Lett.* 110 (21) (2013) 210603.
- [20] T. Vogel, Y. W. Li, T. Wüst, D. P. Landau, *Phys. Rev. E* 90 (2) (2014) 023302.
- [21] J. Zierenberg, M. Marenz, W. Janke, *Comput. Phys. Commun.* 184 (4) (2013) 1155–1160.
- [22] J. Gross, J. Zierenberg, M. Weigel, W. Janke, *Comput. Phys. Commun.* 224 (2018) 387–395.
- [23] Y. W. Li, M. Eisenbach, in: *Proceedings of the Platform for Advanced Scientific Computing Conference, PASC '17*, ACM, New York, NY, USA, 2017, pp. 10:1–10:7.
- [24] B. A. Berg, R. C. Harris, *Comput. Phys. Commun.* 179 (6) (2008) 443–448.
- [25] A. N. Kolmogorov, *Giornale dell'Istituto Italiano degli Attuari* 4 (1933) 83–91.
- [26] N. Smirnov, *Rec. Math. [Mat. Sbornik]* 6 (48) (1939) 3–26.
- [27] Y. W. Li, T. Wüst, D. P. Landau, H. Q. Lin, *Comput. Phys. Commun.* 177 (6) (2007) 524–529.
- [28] M. A. Stephens, *J. Royal Stat. Soc. Series. B* 32 (1) (1970) 115–122.
- [29] B. A. Berg, *Markov Chain Monte Carlo Simulations and Their Statistical Analysis*, World Scientific Publishing, Singapore, 2004.
- [30] D. B. Owen, *Handbook of Statistical Tables*, Addison–Wesley Publishing, 1962.
- [31] *Mathematica*, version 11.0.1, Wolfram Research, Inc., Champaign, Illinois, U.S.A. (2016).